Space and time analysis of the solar photospheric dynamics at moderate ℓ values

M. Oliviero, G. Severino, and Th. Straus
Osservatorio Astronomico di Capodimonte, Via Moiariello 16, I-80131 Napoli, Italia

S. M. Jefferies
National Solar Observatory, P.O. Box 26732, Tucson, USA
and

T. Appourchaux
Space Science Department, ESA, ESTEC, Postbus 299, NL-2200 AG Noordwijk, The Netherlands

ABSTRACT

A space-time analysis of thirty-six days worth of full-disk intensity and velocity images, obtained by the Global Oscillation Network Group (GONG), is used to produce a high resolution $\ell - \nu$ phase difference spectrum for the spectral range ($4 \leq \ell \leq 200$, $0 \leq \nu \leq 8.3$ mHz). This is the first time a phase difference spectrum has been produced for intermediate ℓ-values.

The phase differences on the p-mode ridges are found to linearly increase from $\sim 65°$ at 2 mHz up to $\sim 95°$ at 4.7 mHz. Only near 3.9 mHz are the differences close to 90°: the theoretically expected phase for adiabatic evanescent waves. The phases between the ridges exhibit a step-like behavior in frequency with negative values at low frequency, and positive values (greater than 90°) at high frequency. The negative phase values are consistent with the extension to low and moderate ℓ-values of the plateau-interridge regime discovered by Deubner et al. (1990). However, positive phase values, which represent higher phase for the solar background than for the acoustic modes, were not expected. An understanding of this observed phase difference behavior will improve our knowledge of the nature of the solar background and its interaction with the acoustic p-modes.

Subject headings: Sun: atmospheric motions, oscillations, photosphere

1. Introduction

The space and time analysis of intensity (I) and velocity (V) fluctuations observed in a single photospheric line, provides I and V power and I−V phase differences corresponding roughly to the same level in the solar photosphere. This information can be used to understand the physical processes that cause the observed fluctuations. For instance, in a gravitationally stratified one dimensional atmosphere - among the linear adiabatic waves whose amplitudes are stationary in time - evanescent waves have a temperature-velocity phase difference of 90°, outgoing progressive waves have phases between 0° and 90°, and ingoing waves have phases between 90° and 180°. To date, phase difference analyses have been used to study the dynamics of the solar atmosphere using high-resolution, disk center observations (e.g., Deubner et al. 1992, Deubner 1998) and unimaged, Sun-as-a-star, observations (e.g., Schrijver et al. 1991, Jiménez et al. 1998). These types of observations allow phase difference measurements to be made at high- and low-ℓ values. Up until now, phase diagrams have not been applied to the intermediate ℓ values that are measured by observations of the resolved full solar disk (Oliviero et al. 1998, Masiello et al. 1998). Considering the potential of phase diagnostics to determine the dynamics of the solar atmosphere, this is a serious omission. In this Letter we describe a first step towards correcting this problem.

2. Data analysis

The data used for our study are the product of the decomposition of GONG velocity and intensity images into spherical harmonics for the degree and azimuthal order ranges $4 \leq \ell \leq 200$ and $-\ell \leq m \leq \ell$, respectively. Due to the significant sensitivity of the intensity signal to atmospheric noise (Jiménez et al. 1987, Andersen & Domingo 1988) we excluded the low-ℓ spectra ($\ell \leq 3$) from our analysis. The data set represents observations made during the period March 21 to April 25, 1997, and has a duty cycle of 79%. To achieve the best signal-to-noise on the modes in both the power and phase spectra of the time series of the spherical harmonic coefficients, it is important to remove the effects of solar rotation. Solar rotation causes the observed modal features in the spectra to be shifted in frequency by an amount

$$\Delta\nu_{\rm rot}(\ell, m) = -L \sum_{i=1}^{5} a_i P_i(-m/L) \ , \qquad (1)$$

where $L = \sqrt{\ell(\ell+1)}$ and P_i are the Legendre polynomials of degree i (Duvall et al. 1986). We corrected the spherical harmonic coefficients for the effects of rotation by multiplying each coefficient by $\exp[-i\, 2\pi \Delta\nu_{\rm rot}(\ell, m) t]$. This method of rotation correction avoids the need for delicate interpolation of the power and phase spectra. However, it does assume that the dependence of the a_i coefficients on both the radial order, n, and degree is small. The latter assumption starts to break down for ℓ values less than ∼40. We used the values[1]: $a_1 = -413.6\,$nHz; $a_2 = 7.8\,$nHz; $a_3 = -21.2\,$nHz; $a_4 = 2.9\,$nHz; $a_5 = 4.1\,$nHz.

We computed the $\ell - \nu$ spectra for the intensity power ($P_{\rm I}$), velocity power ($P_{\rm V}$), phase difference ($\Phi_{\rm I-V}$), and coherence (COH), using the relations

$$P_{\rm I,V}(\ell, \nu) = \sum_{m=-\ell}^{\ell} |T_{\rm I,V}(\ell, m, \nu)|^2 \qquad (2)$$

$$\Phi_{\rm I-V} = \arg \sum_{m=-\ell}^{\ell} T_{\rm I}(\ell, m, \nu) T^*_{\rm V}(\ell, m, \nu) \qquad (3)$$

$$\mathrm{COH} = \frac{\left| \sum_{m=-\ell}^{\ell} T_{\rm I}(\ell, m, \nu) T^*_{\rm V}(\ell, m, \nu) \right|}{\left[\sum_{m=-\ell}^{\ell} \left| T_{\rm I}(\ell, m, \nu) T^*_{\rm V}(\ell, m, \nu) \right| \right]} \ . \qquad (4)$$

Here $T_{\rm I}(\ell, m, \nu)$ and $T_{\rm V}(\ell, m, \nu)$ are the Fourier transforms of the rotation corrected intensity and velocity coefficients, and $*$ denotes the complex conjugate quantity. The degree and frequency resolutions of the spectra are $\Delta\ell \sim 3$ (Howe and Thompson 1998) and $\Delta\nu \sim 0.3\,\mu$Hz respectively. These resolutions are superior to those used in previous phase difference analyses.

3. Results and discussion

Figure 1 shows a slice through the resulting spectra for $\ell = 200$. For the following discussion we assume that: (a) the $\ell = 200$ spectra are representative of the full ℓ−ν diagrams, and (b) the observed signal has two

[1]These are the default values given in the routine ROTCOR of the GRASP/GONG package (January, 1993).

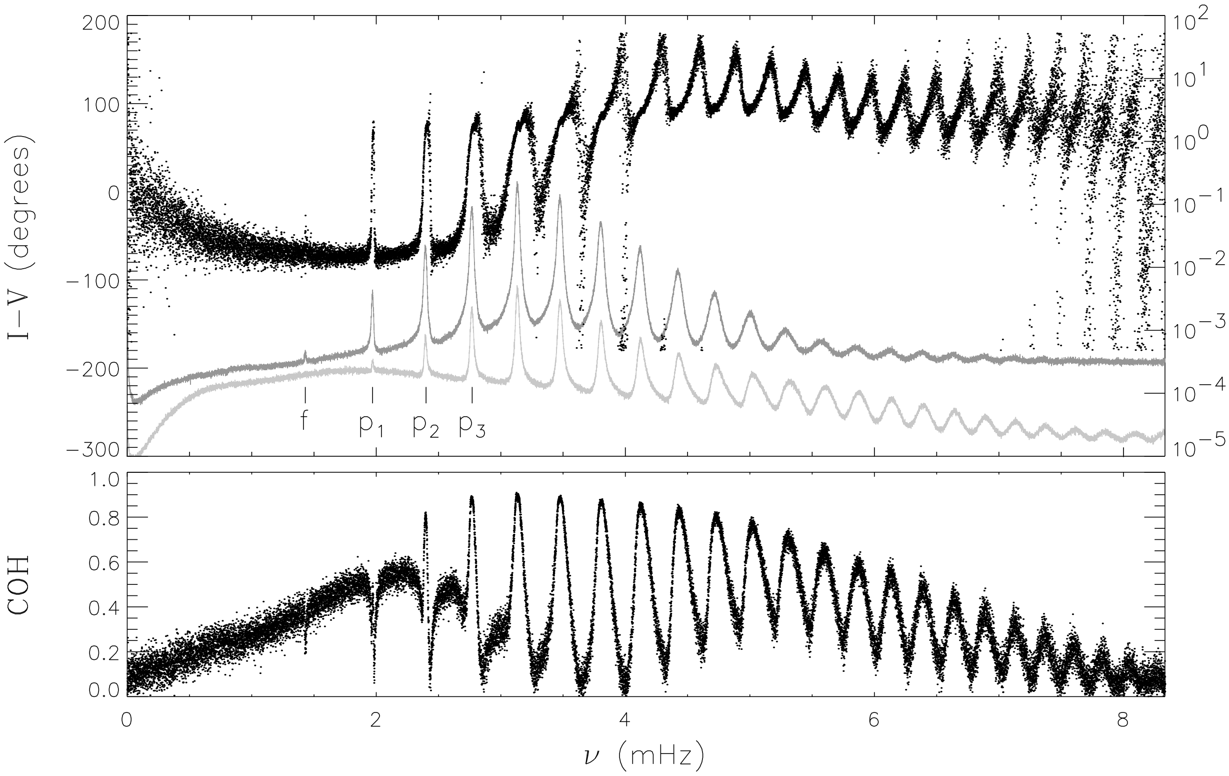

Fig. 1.— Phase difference I−V (upper panel, black points) and coherence COH (lower panel, black points) at $\ell = 200$. In the upper panel are also plotted the velocity (dark grey line) and intensity (light grey line) power spectra in arbitrary units (right axis).

components: a p-mode signal, and a solar background signal. In the neighborhood of p-modes, we define the background signal to be the signal between the ridges of modal power. Figure 2 shows the frequency variation of the measured phase and coherence for these two components for all ℓ values. As can be seen, the ℓ variation of the measured parameters is small compared to the frequency variation. The ℓ dependence of the phase difference deserves special attention at low ℓ, where the GONG intensity data are noisy. We note that Jiménez et al. (1998), using space-based data, measure a decrease in the phase difference as ℓ increases from 0 to 3.

We will first examine the behavior of the solar background signal. At frequencies between 1 and 2 mHz the phase difference of the solar background signal is essentially constant with frequency ($\Phi_{\rm I-V} \simeq -70°$). This "plateau" in phase is independent of ℓ and continues between the p-modes up to ~ 3.3 mHz. Clearly, this negative phase represents the extension to lower ℓ values of the plateau−interridge regime, first discovered by Deubner et al. (1990) and recently confirmed by Straus et al. (1998). Below $\nu = 1$ mHz the background phase increases with decreasing frequency. Between 3.3 and 4 mHz, the background I−V phase passes from a negative to a positive phase regime in which the background phases are actually greater than the phases for the p-modes. Above 4 mHz the values of the high-frequency background phase peaks vary slowly with ν and ℓ. The coherence for the background signal has two maxima at 2 mHz and 5 mHz (Fig. 2). These maxima coincide with the centers of the negative and positive phase backgrounds, respectively. Since the coherence is a measure of the statistical significance of the phase at a given frequency, this suggests that the negative and positive regimes for the background phase differences are significant. We note that the decreasing trend in COH below 2 mHz might be an effect of seeing or of the time differential filter used by GONG in the

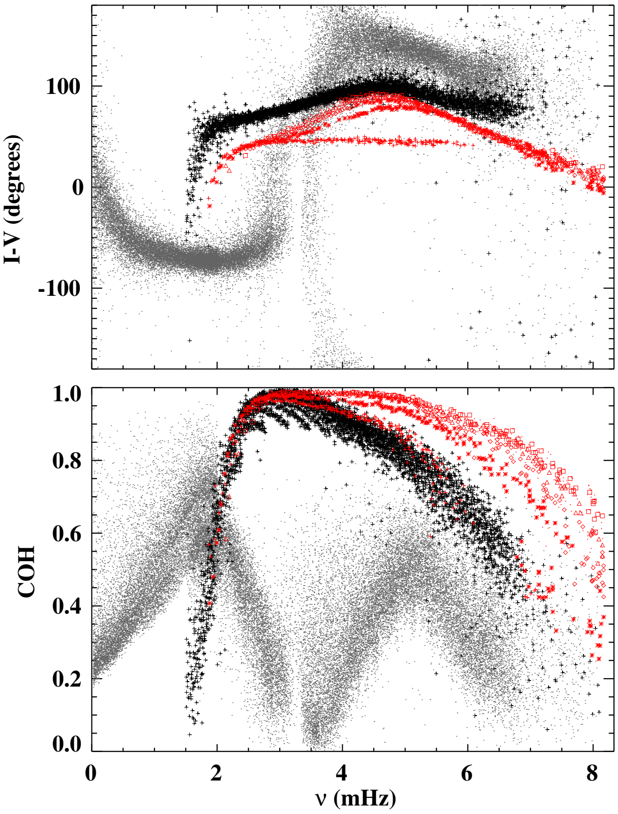

Fig. 2.— Phase difference I−V (upper panel) and coherence COH (lower panel) of the p-mode ridges and in the background. The p-mode phases are computed at the frequencies of the velocity power maxima: black crosses correspond to the current data ($4 \leq \ell \leq 200$), and red symbols to the MDI data ($\ell \gtrsim 200$) of Straus et al. (1999). Background values are calculated only for the GONG data (grey dots).

calculation of the spherical harmonic coefficients.

For the p-mode component of the signal, the I−V phases corresponding to the p-mode frequencies increase almost linearly with frequency over the range 2−5 mHz: passing from $\sim 65°$ at 2 mHz up to $\sim 95°$ at 4.7 mHz. This linear trend is essentially independent of degree over the range $4 \leq \ell \leq 200$. Phase differences on the modes below 90°, the expected phase for adiabatic evanescent waves, have been interpreted as due to the physical mixing between the modes and the underlying background (Severino et al. 1998, Nigam & Kosovichev 1999). Our results provide further evidence to support this idea. When the mixing with the background is more effective, e.g., when

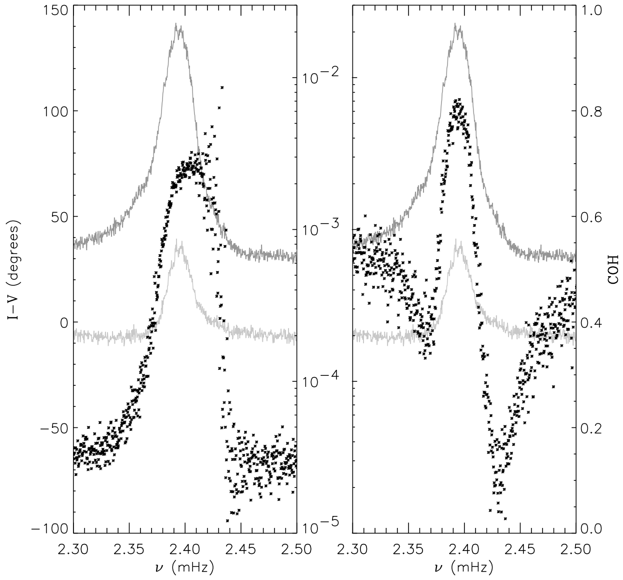

Fig. 3.— Phase difference I−V (left panel) and coherence (right panel) around the p_2 ridge at $\ell = 200$. In both panels are plotted also the I and V power spectra. Line coding as in Figure 1.

the oscillation-to-background signal ratio is low, the solar oscillations have lower phase differences. This is also supported by a comparison in Figure 2 of GONG phase differences with MDI phases (Straus et al. 1999) which have a factor of 60 in frequency and a factor of 5 in degree, lower resolution. On the other hand, if the oscillation-to-background signal ratio is high, then $\Phi_{\rm I-V}$ should be close to 90° on the modes. This is observed in the GONG phases over the frequency interval 3.7-4.1 mHz, where the coherence level of the background signal reaches its minimum value. This result is independent of ℓ value. We speculate that another demonstration of the mode-background interaction is provided by the ℓ dependence of the interridge/background phase maxima at high frequency. This trend may be due to the smaller separation of the p-mode ridges at lower degree values. That is, as the frequency spacing between the ridges decreases, the overlapping of the tails of the p-mode line profiles becomes stronger and thus reduces the background phase difference in the interridge region. Two other important facets of the phase difference and coherence measurements, for the p-mode profiles below 3.5 mHz, are shown in Figure 3: (1) $\Phi_{\rm I-V}$ has a typical "shark fin" shape, which differs from both V and I power profiles, and (2) The co-

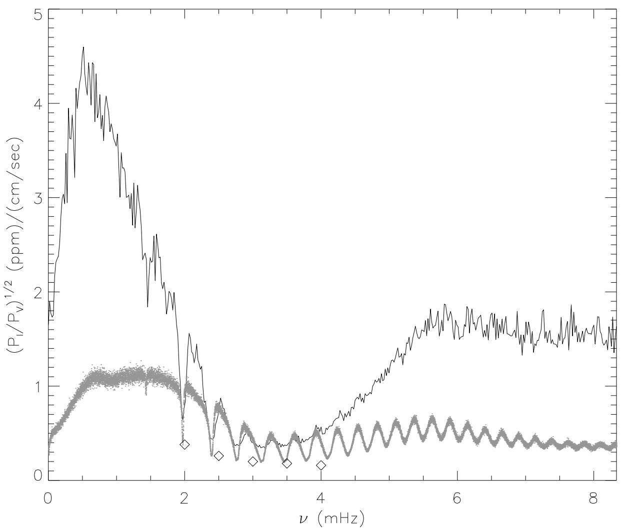

Fig. 4.— Gain for $\ell = 200$. Grey dots refer to GONG data. The MDI data (solid line, Straus et al. 1999), and an average of the Libbrecht (1990) results (diamonds) are shown for comparison.

herence has two asymmetric dips in the wings of the mode peaks, with the deepest dip on the high frequency side. These characteristics may be affected by the ℓ-leakage as well as by the asymmetries of the I and V mode profiles.

Theoretical interpretation of the complex behavior of the $\Phi_{\text{I}-\text{V}}$ spectrum is limited. Gough (1985) and Houdek et al. (1995) have shown that models of p-modes that include a time dependent mixing length prescription for convection, can produce I$-$V phases on the modes lower than the adiabatic value. Deubner et al. (1992) proposed an explanation for the negative phase background in terms of coherent evanescent oscillations which are the result of continuous partial reflection and scattering of ordinary p-modes. Rast (1999) speculates that the intensity background signal in the frequency range corresponding to the negative $\Phi_{\text{I}-\text{V}}$ regime - i.e. the "plain" component of Straus et al. (1999) - may be directly related to the excitation mechanism for the acoustic modes. Obviously a fundamental question that needs to be answered is: "What is the physical interpretation of the solar background signal $-$ convection or waves?". In an attempt to answer this question, we analysed synthetic temperature (T) and velocity data produced by a two-dimensional, fully compressible, convective model (Steffen 1991). Preliminary $\Phi_{\text{T}-\text{V}}$ spectra of these data show quantitative agreement with the negative phase regime in the $\Phi_{\text{I}-\text{V}}$ spectra for real data. However, a theoretical compressible model produces signals for both waves and convection, which, unfortunately, are not easy to separate. Two further complications are that: (1) it is difficult to distinguish between model resonances and background, and (2) temperature is not necessarily a good proxy for intensity over any frequency range (Severino et al. 1998).

Figure 4 shows the intensity to velocity amplitude ratio, or "gain", as a function of frequency. The gain is of particular interest for the GONG data because it is unaffected by the first differential filter. This filter, which is used to reduce the non-solar noise at low frequency, also suppresses the I and V solar signals in the same frequency range. In the middle of the p-mode frequency range, the gain minima correspond to the p$-$mode frequencies, while the gain maxima occur between the modes. The gain for low and intermediate modes depends only weakly on frequency in the range between 2 and 4 mHz. In a gravitationally stratified one dimensional atmosphere, there are two kinds of linear adiabatic evanescent waves whose amplitudes are stationary in time. One type has energy density decreasing with height and gain increasing with frequency, the other has energy density increasing with height and gain decreasing with frequency. Thus, the measured gain data seem to indicate that both the p-modes and the background - if it can be described in terms of waves $-$ have an energy density that is predominantly increasing with height in the photosphere.

In conclusion, a better theoretical understanding of phase diagnostics is required before we are able to fully realize the potential of this tool for defining the dynamical character of the observed wave fields. This is not an easy task as the solar photosphere is a relatively thin boundary layer between the convective interior and the optically thin and magnetic atmosphere into which convection overshoots and different kinds of waves are excited and damped. Such a system cannot be described with a simple dynamical model. However, the high-quality phase measurements presented here, and future measurements that are inevitable with the excellent data being collected by the GONG and MDI experiments, will surely spur such an effort.

This work utilizes data obtained by the Global Oscillation Network Group (GONG) project, managed by the National Solar Observatory, a Division of the National Optical Astronomy Observatories, which is operated by AURA, Inc. under a cooperative agreement with the National Science Foundation. The data were acquired by instruments operated by the Big Bear Solar Observatory, High Altitude Observatory, Learmonth Solar Observatory, Udaipur Solar Observatory, Instituto de Astrofísica de Canarias, and Cerro Tololo Interamerican Observatory. We thank John Leibacher for his comments on the manuscript.

REFERENCES

Andersen, B. N., & Domingo, V. 1988, IAU Symposia, 123, 67

Deubner, F.-L. 1998, IAU Symposia, 185, 427

Deubner, F.-L., Fleck, B., Marmolino, C., & Severino, G. 1990, A&A, 236, 509

Deubner, F.-L., Fleck, B., Schmitz, F., & Straus, Th. 1992, A&A, 266, 560

Duvall, T. L., Jr., Harvey, J. W., & Pomerantz, M. A. 1986, Nature, 321, 500

Gough, D. 1985, ESA SP-235, 183

Houdek, G., Balmforth, N. J., & Christensen-Dalsgaard, J. 1995, ESA SP-376, Vol. 2, 447

Howe, R., & Thompson, M. J. 1998, A&AS, 131, 539

Jiménez, A., et al. 1987, A&A, 172, 323

Jiménez, A., et al. 1998, ESA SP-418, in press

Libbrecht, K. G. 1990, ApJ, 359, 232

Masiello, G., Marmolino, C., & Straus, Th. 1998, ESA SP-418, in press

Nigam, R., & Kosovichev, A. G. 1999, ApJ, 510, L149

Oliviero, M., Severino, G., & Straus, Th. 1998, ESA SP-418, in press

Rast, M. P. 1999, private communication

Schrijver, C. J., Jiménez, A., & Dappen, W. 1991, A&A, 251, 655

Severino, G., Straus, Th., & Jefferies, S. M. 1998, ESA SP-418, in press

Steffen, M. 1991, NATO ASI-Series C, 341, 263

Straus, Th., Fleck, B., Severino, G., Deubner, F.-L., Marmolino, C., & Tarbell, T. 1998, ESA SP-417, 293

Straus, Th., Severino, G., Deubner, F.-L., Fleck, B., Jefferies, S. M., & Tarbell, T. 1999, ApJ, 516, in press